

Visual Quality Improvement of Watermarked Image Based on Singular Value Decomposition Using Walsh Hadamard Transform

Aris Marjuni¹, Ahmad Zainul Fanani¹, Oky Dwi Nurhayati²

¹Department of Informatics Engineering, Universitas Dian Nuswantoro, Semarang, Indonesia

²Department of Computer Engineering, Universitas Diponegoro, Semarang, Indonesia

E-mails: aris.marjuni@dsn.dinus.ac.id a.zainul.fanani@dsn.dinus.ac.id okydwin@gmail.com

Abstract: Embedding the watermark is still a challenge in image watermarking. The watermark should not reduce the visual quality of the image being watermarked and hard to distinguish from its original. Embedding a watermark of a small size might be a good solution. However, the watermark might be easy to lose if there is any tampering with the watermarked image. This research proposes to increase the visual quality of the watermarked image using the Walsh Hadamard transform, which is applied to the singular value decomposition-based image watermarking. Technically, the watermark image is converted into a low bit-rate signal before being embedded in the host image. Using various watermark sizes, experimental results show that the proposed method could produce a good imperceptibility with 47.10 dB on average and also gives robustness close to the original watermark with a normalized correlation close to 1 on average. The proposed method can also recognize the original watermark from the tampered watermarked image at different levels of robustness.

Keywords: Image watermarking, Image authentication, Imperceptibility and robustness, Singular value decomposition, Walsh-Hadamard transform.

1. Introduction

A digital image, which is referred to as an image, is one of the important multimedia content in the current digital era. Images are not only used in the arts and photography but are also widely used as information or data. Some applications such as e-commerce, blogs, websites, mobile applications, profiles, and many more, need images to enrich the application content. Imaging technology made it easy for anyone to create, store, publish or distribute digital images. However, it also leads to any kind of infringements, such as falsification, manipulation, and duplication with an illegal operation. If the digital image has personal property rights, it is necessary to be protected by ownership protection or image authentication to avoid any kind of abuse. Although the protection cannot be fully guaranteed, at least the owner could still provide authentication of ownership as a legal rights owner. One of the techniques to provide image authentication is digital image watermarking [1].

A watermark is digital content embedded in the host or original image, which is usually small in size and contains any ownership information [2]. Besides, the watermark could also be recovered to prove the authentication when an infringement happens on the original image [3]. In the image watermarking technique or scheme, there are at least two processes that are watermark embedding and watermark extraction or recovery. The effectiveness of the image watermarking techniques is usually evaluated by the following two requirements, which are imperceptibility and robustness. Imperceptibility means that the watermark should not reduce the visual quality of the image being watermarked and an observer cannot make enough distinction between the watermarked image from its original. While robustness means that the watermark should not be lost by any kind of image processing from unauthorized parties. The imperceptibility and robustness are trade-off constraints that usually conflict with each other, where increasing the imperceptibility will decrease the robustness and vice versa [4].

The image watermarking schemes can be classified into two main categories, which are spatial domain and transform domain schemes [4, 5]. A Least Significant Bit is an example algorithm in the spatial domain that modifies the low-order bits of the host image for the embedding process [6]. Whereas some algorithms such as the discrete cosine transform [7], discrete Fourier transforms [8], and discrete wavelet transform are algorithms mostly based on the frequency domain [9]. The Singular Value Decomposition (SVD) is another transform that uses the component matrices obtained by SVD for watermark image embedding. The SVD transform become popular in image watermarking as this transform can produce simplified components that make the watermarking process to be done easily.

The SVD image watermarking has been proposed in many previous works with many improvement efforts. The SVD image-watermarking scheme through the chaotic map has been proposed in [10]. The embedding watermark into the SVD domain for protecting rightful ownership through key mapping and coefficient ordering is also proposed in [11]. An SVD image watermarking algorithm using a value ordering scheme has been proposed in [12]. Some hybrid methods based on SVD image watermarking have also been proposed in other domains. The SVD hybrids with lifting wavelet transform have been proposed in [13], SVD hybrids with Discrete Wave Transformation (DWT) and Hessenberg decomposition have been proposed in [14], and also SVD hybrids with lifting scheme on SVD and Schur Decomposition are proposed in [15]. The other existing hybrid schemes on SVD have been also observed in [16] through their survey, where the SVD algorithm has been widely combined with some methods such as invariant wavelet, particle swarm optimization, human visual system, genetic algorithm, evolutionary algorithm, firefly algorithm, artificial bee colony, and k-Means Algorithm to achieve better performance.

Based on the state of the art and related works of the existing SVD image watermarking above, we propose an improved SVD image watermarking through Walsh-Hadamard (WH) transform, mainly in both imperceptibility and robustness. The basic idea of this proposed method is that the Walsh-Hadamard transform can be used to convert the watermark into a low bit rate of a signal. Thus, the watermarked

image can be expected more imperceptible because only a small bit of the signal would be inserted into the original image. Besides, this research also presents a robustness analysis to evaluate the resilience of watermarks against image tampering caused by noise insertion, cropping, rotation, compression, and resizing.

This paper is presented in several sections, which are: Theoretical review – Section 2; Proposed method – Section 3; Experimental setup – Section 4; Result and analysis – Section 5; Conclusion – Section 6. The literature review section presents a brief of the basic theories, including the singular value decomposition and the Walsh Hadamard function. The proposed method section presents the proposed image watermarking method, including watermark embedding and watermark extraction. The experimental setup section presents the image data preparation, the image watermarking process as an experimental design, and the performance evaluation. The results and analysis section presents the experimental results based on the proposed method and experimental design. This section also includes a discussion about the performance evaluation of the proposed method, especially for imperceptibility and robustness. While the conclusion of this study is summarized in the conclusion section, including the limitations and suggestions for further study.

2. Theoretical review

2.1. Singular Value Decomposition (SVD)

SVD is a factorization method for decomposing a matrix into component matrices that contain singular values and singular vectors. SVD provides an easy way to divide a matrix, which might consist of some data in simpler matrices. Let I be the $N \times N$ of real matrix R with rank r , where $r \leq N$. The SVD of the matrix I is formulated in the next equation as a factorization of eigendecomposition matrices U , S , and V [15] as follows:

$$(1) \quad \begin{aligned} f_{\text{SVD}}(I) &= [U, S, V], \\ I &= U \times S \times V^T, \end{aligned}$$

where S is a singular matrix that contains descending ordered singular values (s_1, s_2, \dots, s_N), U is a left singular vector (u_1, u_2, \dots, u_N), V is a right singular vector (v_1, v_2, \dots, v_N), while V^T is a matrix transpose of V . The SVD of an image I represents the relation between three matrices, which are: U , S , and V satisfying both $Iv_i = s_i u_i$ and $u_i^T I = s_i v_i^T$ where $u_i \in U$, $s_i \in S$, and $v_i \in V$, and $s_1 \geq s_2 \dots \geq s_r \geq s_{r+1} = s_{r+2} = s_N = 0$ as shown in the next equation [17]:

$$(2) \quad \begin{aligned} I &= \begin{bmatrix} u_1 & u_2 & \dots & u_N \end{bmatrix} \begin{bmatrix} s_1 & 0 & \dots & 0 \\ 0 & s_2 & \dots & 0 \\ \vdots & \vdots & \ddots & \vdots \\ 0 & 0 & \dots & s_N \end{bmatrix} \begin{bmatrix} v_1 & v_2 & \dots & v_N \end{bmatrix}^T = \\ &= \sum_{i=1}^r s_i u_i v_i^T = s_1 u_1 v_1^T + s_2 u_2 v_2^T + \dots + s_r u_r v_r^T. \end{aligned}$$

In image processing analysis, the digital image can be represented as a matrix. Regarding the use of SVD in image processing, the digital image can be converted

into a matrix for analytical purposes and all of the pixel values will be used directly as matrix elements. For example, Lena image I of 512×512 is decomposed into U , S , and V images, and these images can be reconstructed back to the original image using (1) by multiplication of U , S , and V^T using the rank approximation r of the image I . The matrix S represents the main component of the image I , which means that the matrix S reflects important information about image I .

The singular values are relatively stable in almost all image processing, so there is no large change or variation in its SVD. This characteristic makes SVD more powerful in image processing. Whereas, the matrices U and V restrain the image through the multiplication of U and V^T [16]. Fig. 1 illustrates reconstructed images after the SVD decomposition of Lena with r of 8, 16, 32, and 64, respectively. It shows that using the higher-rank approximation will result in more perceptible image reconstruction, and mainly, with the maximum rank will reconstruct the original image perfectly.

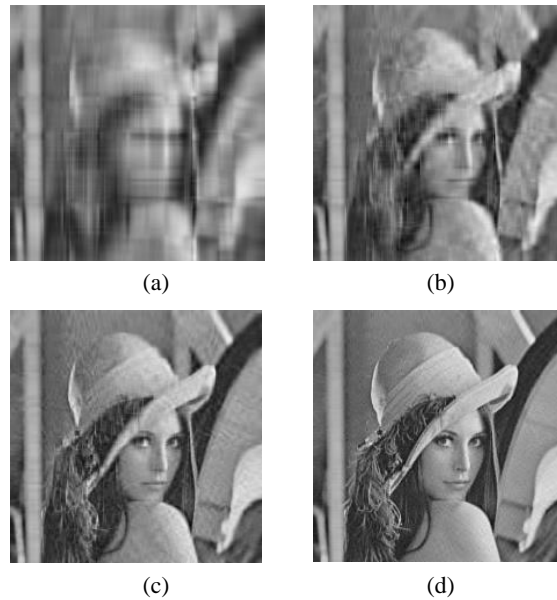


Fig. 1. Reconstructed image of Lena using SVD with rank approximations: $r=8$ (a), $r=16$ (b), $r=32$ (c), and $r=64$ (d)

2.2. Walsh-Hadamard transform

The Hadamard transform, usually called Walsh Hadamard (WH) transform, is constructed on a square wave with 1 and -1 as maximum and minimum element values, respectively. This transformation is an efficient computation because it only consists of the 1 and -1 elements [18]. The smallest Hadamard matrix is H_1 and is defined in the next equation [19] as

$$(3) \quad H_1 = \frac{1}{\sqrt{2}} \begin{bmatrix} 1 & 1 \\ 1 & -1 \end{bmatrix}.$$

The Hadamard matrix of ordo N or H_N can be constructed by the Kronecker product H_1 and H_{N-1} , where $N=2^n$, and n is an integer number, as formulated:

$$(4) \quad H_N = H_1 \otimes H_{N-1} = \begin{bmatrix} H_{N-1} & H_{N-1} \\ H_{N-1} & -H_{N-1} \end{bmatrix}.$$

If there is a vector x of length N , then the Walsh-Hadamard of x is computed using the next equation as follows:

$$(5) \quad \text{WH}(x) = \frac{1}{N} \sum_{i=0}^{N-1} x_i W(n, i),$$

where $i=0, 1, \dots, N$, and $W(n, i)$ is a Walsh function [20], which is defined as follows:

$$(6) \quad W(n, i) = \begin{cases} \text{Cal}\left(\frac{n}{2}, i\right), & n = 0, 2, 4, \dots, \\ \text{Sal}\left(\frac{n+1}{2}, i\right), & n = 1, 3, 5, \dots, \end{cases}$$

where Cal and Sal functions are computed by H_N in (4).

Generally, if x is a signal vector, X is a spectrum vector, and H_w is the Hadamard matrix, then the WH transform of the signal vector x and its inverse are formulated as:

$$(7) \quad \begin{aligned} \text{WH}(x) &= H_w(x) = X, \\ i\text{WH}(X) &= H_w(X) = x. \end{aligned}$$

The WH and $i\text{WH}$ can also be written as a linear combination [18], as formulated in the next equations, respectively,

$$(8) \quad \begin{aligned} X_w(k) &= \sum_{n=0}^{N-1} x(n) W_N(k, n) = \sum_{n=0}^{N-1} x(n) \prod_{i=0}^{M-1} (-1)^{n_i k_{M-1-i}}, \\ x(n) &= \frac{1}{N} \sum_{k=0}^{N-1} X_w(k) W_N(k, n) = \frac{1}{N} \sum_{k=0}^{N-1} X_w(k) \prod_{i=0}^{M-1} (-1)^{n_i k_{M-1-i}}, \end{aligned}$$

where $N=2^M$, $M=\log_2 N$, $i=0, 1, \dots, M-1$, and $k=0, 1, \dots, N-1$.

3. Proposed method

This research proposes a method for the performance of both, the imperceptibility and robustness of the SVD-based image watermarking to be improved through the WH transform. The proposed method is applied to both watermark embedding and extraction. Watermark embedding is a process to embed the watermark into the host image. Watermark extraction is a process to recover the watermark from the watermarked image with or without tampering. The use of SVD and WH transforms in the proposed method is described as follows.

3.1. Watermark embedding

Suppose image I is an original or host image, while image W is a watermark image. The watermark embedding to insert the watermark W into the host image I is performed by applying SVD and WH transforms through the following steps:

a. Decompose image I into S , U , and V by SVD transform to get the singular value of I using Equation (1).

b. Modify the watermark image W and singular matrix S by WH transform to get a new signal vector of W' and S' , as formulated in Equation (5).

c. Embed the signal vector W to the singular value S using the scale factor α [21] and construct the new singular value S_I as formulated in the next equation,

$$(9) \quad S_I = S + \alpha \times W'.$$

The scale factor α is a positive constant that is used to adjust the strength level of the inserted watermark.

d. Perform the inverse of WH transform on S_I using the Equation (7) to get S_I' ,

$$(10) \quad S_I' = iWH(S_I).$$

e. Decompose S_I' in the Equation (10) into U_w , S_w , and V_w by SVD transform to get the singular value of S_I' using the Equation (1),

$$(11) \quad f_{\text{SVD}}(S_I') = [U_w, S_w, V_w].$$

f. Reconstruct the watermarked image I' using the Equation (1) based on the singular value S_w in the Equation (11) as follows:

$$(12) \quad I' = US_w V^T.$$

3.2. Watermark extraction

Suppose image I' is a watermarked image with $M \times M$ in size. The watermark extraction from the watermarked image I' is explained as follows.

a. Decompose I' by SVD transform into S' , U' , and V' matrices to get the singular value of I' using the Equation (12),

$$(13) \quad \text{SVD}(I') = [U', S', V'].$$

b. Obtain the Estimated singular value S_E that contains the watermark using the inverse of the SVD transform using the Equation (13),

$$(14) \quad S_E = U_w S' V_w^T.$$

c. Perform WH transform on S_E using the Equation (5) as in Equation (14),

$$(15) \quad S_E' = WH(S_E).$$

d. Extract the estimated watermark by subtracting the singular values S_E' and S with the same scale factor α using the Equation (15):

$$(16) \quad W' = (S_E' - S) / \alpha.$$

e. Reconstruct the estimated watermark by the inverse of the WH transform using the Equation (9) as in Equation (16),

$$(17) \quad W_E = iWH(W').$$

4. Experimental setup

This research uses a quantitative approach that focuses on verifying the proposed image watermarking method by measuring performance parameters, such as imperceptibility and robustness parameters. The imperceptibility parameter is used to evaluate the visual quality of the proposed image watermarking scheme, which is measured by the peak signal-to-noise ratio. While the robustness parameter is used to evaluate the resilience of the proposed image watermarking scheme, which is measured by normalized cross-correlation. The image watermarking method in this research is applied for image authentication, which means that the proposed method

can be used to evaluate image authenticity by assessing the recovered watermark from the tampered watermarked image. The common test image data for a case study and the details of the research method are described as follows.

4.1. Image data preparation

This study uses a Lena as a host or original image that is a grayscale image of 512×512 sizes. While the Cameraman image is used as a watermark image that is a grayscale image of 256×256 sizes [10]. This watermark image generally can be personal or individual content for authentication marks or ownership. Both these original and watermark images are presented in Fig. 2.

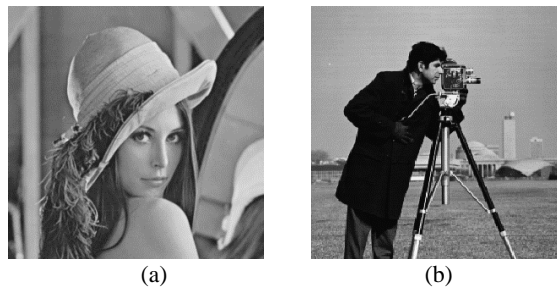


Fig. 2. Host image Lena (a), Watermark image Cameraman (b)

4.2. Image watermarking process

The experimental study has been conducted based on the two image watermarking scheme processes, which are presented in Fig. 3 and include the following steps:

- Watermark embedding – this step is performed to insert the watermark into the host image by following the watermark embedding algorithm that is described in Section 3.1. The output of this process is a watermarked image.

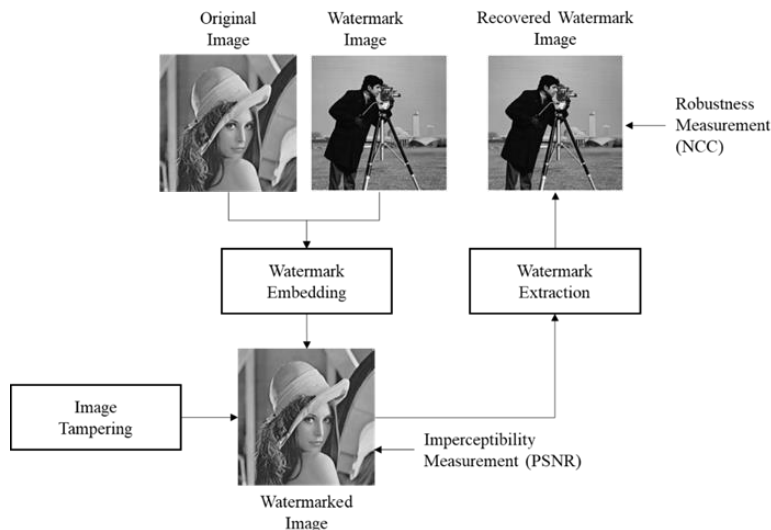


Fig. 3. Image watermarking process

- Watermarked extraction – this step is performed to recover the watermark from the watermarked image with/without tampering by following the watermark extraction algorithm in Section 3.2. In case of tampering, some common attacks in image processing such as image noising, rotation, compression, cropping, and resizing are applied to the watermarked image before extraction. Some parameters may be used on each attack to ensure the resilience of watermarked images under different conditions. The output of this process is a recovered watermark image.

4.3. Performance evaluation

To evaluate the performance of the method being proposed, this study uses imperceptibility and robustness measurements [22]. The Peak Signal-to-Noise Ratio (PSNR) in (18) is used to measure the watermarked image imperceptibility with/without tampering [23]. This metric represents image quality after it is reconstructed, restored, or corrupted. A high PSNR represents a high visual quality of the watermarked image. Conversely, the low PSNR indicates that the watermarked image is of decreased visual quality due to the changes in the image pixel structure:

$$(18) \text{ PSNR} = 10 \log_{10} \left(\frac{255^2}{\sum_{i=1}^M \sum_{j=1}^N [I(i, j) - I'(i, j)]^2} \right), \quad i = 1, 2, \dots, M, \quad j = 1, 2, \dots, N,$$

The Normalized Cross-Correlation (NCC) in the next equation is used to evaluate the recovered watermark image robustness [15]. This metric measures the similarity between the recovered watermark and the original watermark images. A high NCC represents a high similarity of the recovered watermark to its original:

$$(19) \quad \text{NCC} = \frac{\sum_{i=1}^M \sum_{j=1}^N W(i, j) W'(i, j)}{\sum_{i=1}^M \sum_{j=1}^N W(i, j)^2}, \quad i = 1, 2, \dots, M, \quad j = 1, 2, \dots, N,$$

where I is the original image, I' is the watermarked image, W is the original watermark, and W' is the recovered watermark.

5. Results and analysis

Implementation of the proposed method using the host image *Lena* and the watermark image *Cameraman* from Fig. 1 using several embedding scale factors α (0.05, 0.10, 0.15, and 0.20) and watermark sizes (32×32, 64×64, 128×128, and 256×256) are presented in Table 1. The watermarked image quality after embedding the watermark using the proposed method gives 47.10 dB in the PSNR average.

These results show that embedding a less capacity of the watermark image would produce high visual quality. The other factor of visual quality is also affected by the scale factor in the embedding watermark, where the low scale factor will produce high visual quality because only a bit of the watermark will be embedded into the original image. The original image has only a slight decrease in quality due to the additional bits of the watermark. Hence, the quality comparison of the original

and the watermarked images are difficult to distinguish by human eyesight. For example, by using the embedding scale factor $\alpha = 0.2$, with the watermark size of 256×256 , the watermarked image has 33.59 dB, as illustrated in Fig. 4. Visually, the original in Fig. 4a and the watermarked images in Fig. 4d look not different and are difficult to tell apart. However, both images have different rasters affected by image transformation used in the proposed methods, which are SVD and Hadamard transforms. The raster differences between the original and watermarked images are illustrated using histogram and stem plots. The histogram image represents the pixel value distribution of the gray-scale image, while the stem plot represents the scaled pixel value distribution in the range between 0 and 1. The histogram of both original and watermarked images are presented in Fig. 4b and 4e, respectively. While the stem plots of both original and watermarked images are presented in Fig. 4c and 4f, respectively.

Table 1. Watermarked image quality under various embedding scale factors and watermark sizes

Scale factor (α)	Watermark size (row \times column)	Watermark capacity (%)	Watermarked image quality in PSNR (dB)
0.05	32 \times 32	0.39	63.83
0.10	32 \times 32	0.39	55.11
0.15	32 \times 32	0.39	49.74
0.20	32 \times 32	0.39	46.08
0.05	64 \times 64	1.56	58.38
0.10	64 \times 64	1.56	50.33
0.15	64 \times 64	1.56	45.44
0.20	64 \times 64	1.56	42.23
0.05	128 \times 128	6.25	54.64
0.10	128 \times 128	6.25	45.84
0.15	128 \times 128	6.25	41.15
0.20	128 \times 128	6.25	37.97
0.05	256 \times 256	25	50.47
0.10	256 \times 256	25	41.59
0.15	256 \times 256	25	37.18
0.20	256 \times 256	25	33.59
Average			47.10

The being proposed could also recover the embedded watermark from the watermarked image properly with $NCC=1$ under different watermark capacities. This means that the watermark can be recovered from the watermarked image regardless of the size of the embedded watermark.

To evaluate the robustness, further experiments have been performed to measure the resilience of the watermark from tampering, which is measured by the NCC. Several image operations have been performed for robustness evaluation, which are noise insertion, cropping, rotation, compression, and resizing. Noise insertion is a process to add noise generated by a random number generator function. Adding noise to the watermarked image causes visual quality disruption, depending on the noise density. Some noise types are chosen to test the robustness, which is Gaussian noise with zero means ($\mu=0$) and variance σ^2 of 0.5, salt and pepper noise with density δ of 0.05, Poisson noise, and speckle multiplicative noise with variance σ^2 of 0.01. The

recovered watermarks after these noise insertions are illustrated in Fig. 6 with the NCC values are 0.7026, 0.9038, 1, and 0.9085, respectively. Hence, it can be concluded that the proposed image is robust against various noise insertions.

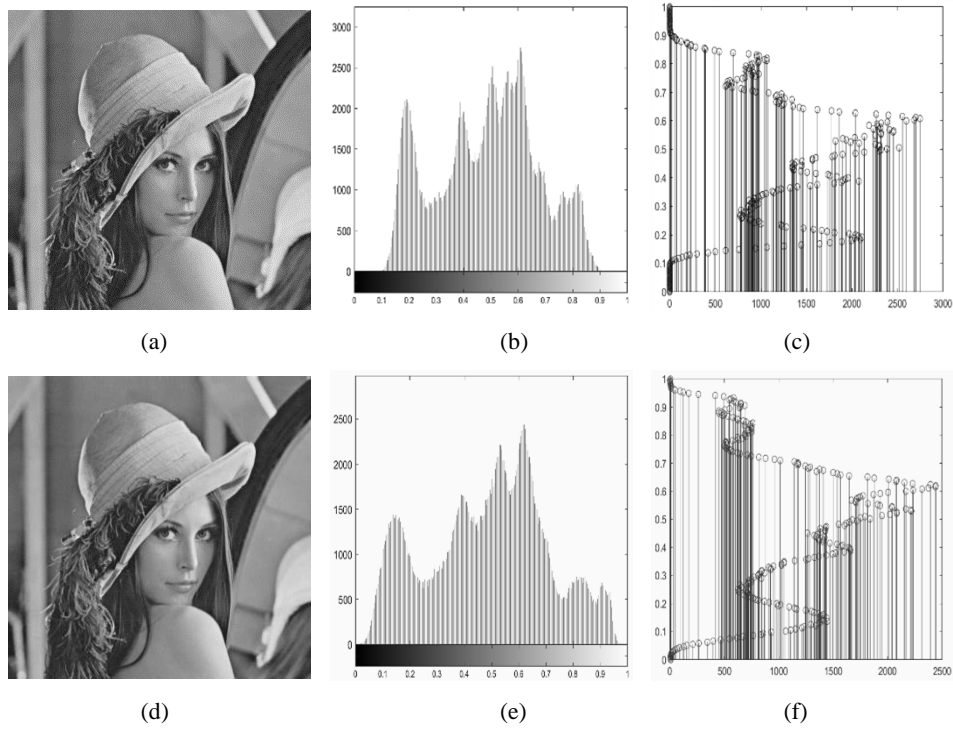


Fig. 4. Host image (a), are histogram and stem plots of host image, respectively, (b) and (c), watermarked image with PSNR=33.59 dB (d), and histogram and stem plots of watermarked image (e) and (f)

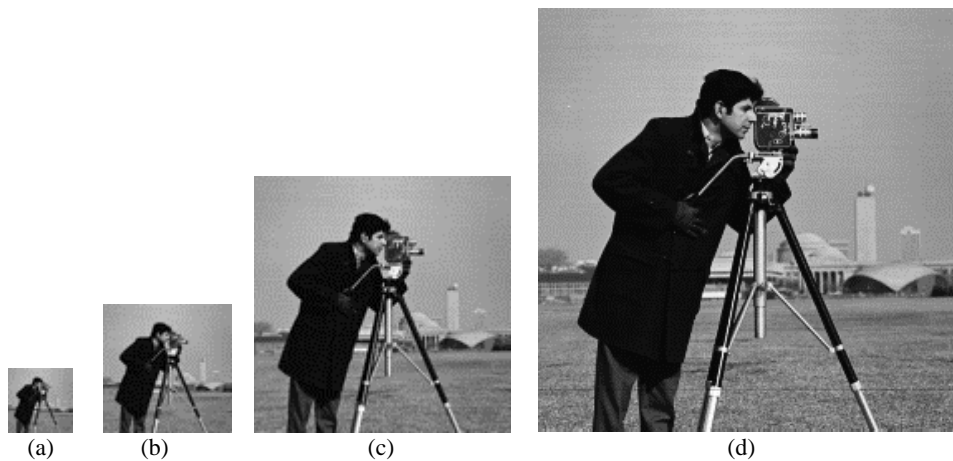


Fig. 5. Recovered watermarked image from watermarked image with $\alpha=0.2$ under different watermark sizes: 32×32 (NCC=1) (a), 64×64 (NCC=1) (b), 128×128 (NCC=1) (c), and 256×256 (NCC=1) (d)

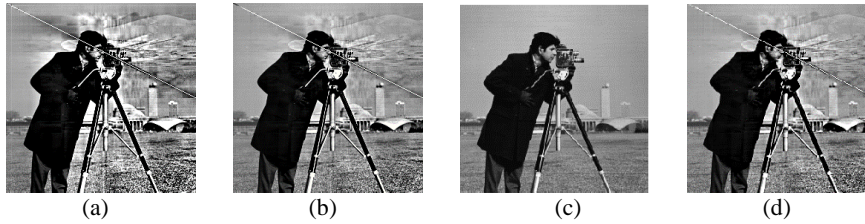


Fig. 6. Recovered watermarked image from the watermarked image with: Gaussian (NCC=0.7026) (a), Salt & Pepper (NCC=0.9038) (b), Poisson (NCC=1) (c), and Speckle (NCC=0.9085) (d)

The next experiment has been evaluating the robustness against image cropping, where the portions of the watermarked image are removed by rows and columns, then the watermark extraction is applied to the disrupted image. In this experiment, the cropping areas (C) have been defined as 6.25%, 12.5%, 25%, and 50% of the watermarked image. For example, if the watermarked image has 512×512 sizes (two dimensions) or $1 \times 262,144$ (one dimension) then the cropped area are 16,384 (6.25%), 32,768 (12.5%), 65,536 (25%), and 131,072 (50%), respectively. The robustness levels of the proposed method after cropping are 0.8002, 0.6677, 0.4540, and 0.3032, respectively. Thus, although there is a part of the watermarked image has cropped, the watermark is also robust and still recovered, as presented in Fig. 7. The NCC of the recovered watermark might decrease because of the geometrical change in the pixel structure. However, the watermark still can be recognized by visual representation from the recovered watermark.

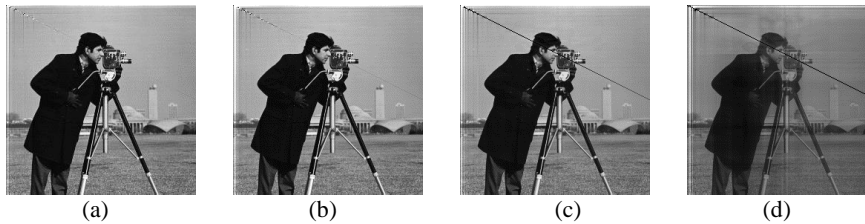


Fig. 7. Recovered watermark from the watermarked image with cropping area: $C=6.25\%$ (NCC=0.8002) (a), $C=12.5\%$ (NCC=0.6677) (b), $C=25\%$ (NCC=0.4540) (c), and $C=50\%$ (NCC=0.3032) (d)

The proposed method is also evaluated against image rotation. The image rotation is a typical attack on the watermarked image using some rotation angle. By the rotation role of a matrix, the output image is larger than the original. In this case, the size of the rotated image is cropped to fit the size of the original matrix. This experiment has used several rotation angles (θ), which are: 30° , 45° , 90° , and 180° . The NCCs of the recovered watermarks are 0.6831, 0.5893, 1, and 1, respectively. Those results show that the NCC with the angle at 90° and 180° have a high coefficient because the watermarked image just changed the position with no cropped areas. The recovered watermark images after image rotation are shown in Fig. 8.

Another experiment to evaluate the robustness of the proposed method is JPEG compression on the watermarked image using a quality factor of compression that represents the degree of loss in the compression. In this experiment, the quality factors Q are 5, 10, 50, and 80. The proposed method could still recover the

watermark from the compressed watermarked image with various visual qualities according to quality factor compressions. A low-quality factor of compression on the watermarked image will give a low quality of the recovered watermark, conversely, a high-quality factor of compression will give a high quality of the recovered watermark close to the original watermark. The examples of the recovered watermark images after JPEG compression are presented in Fig. 9. This means that the proposed method still recovers the watermark clearly at all of those quality factors, hence the proposed scheme is robust against JPEG compressions.



Fig. 8. Recovered watermark from the watermarked image with rotation angle: $\theta=30^\circ$ (NCC=0.6831) (a), $\theta=45^\circ$ (NCC=0.5893) (b), $\theta=90^\circ$ (NCC=1) (c), and $\theta=180^\circ$ (NCC=1) (d)



Fig. 9. Recovered watermark from the watermarked image with JPEG compression: $Q=5$ (NCC=0.9923) (a), $Q=10$ (NCC=0.9974) (b), $Q=20$ (NCC=0.9995) (c), and $Q=80$ (NCC=1) (d)

The last experiment has been evaluating the robustness of the proposed method against image resizing. Image resizing is defined as a new number of rows and columns or $[n_r, n_c]$ that are reconstructed from the watermarked image, including both shrinking and scaling. In this experiment, the watermarked image is resized into $[256 \times 512]$ and $[512 \times 256]$ for shrinking, and $[256 \times 256]$ and $[1024 \times 1024]$ for image scaling. After the extraction process, the results show that the watermarks have high correlation coefficients after the watermarked images are resized, which are 0.9998, 0.9954, 0.9959, and 0.9970, respectively. The watermarked images and recovered watermark images after image resizing are presented in Fig. 10.

The robustness performance average of the proposed method is also compared to the other existing similar methods, particularly to the image watermarking method based on Hadamard Transforms, which SVD and Fast Walsh Hadamard Transform (FWHT) proposed in [11], Principle Component Analysis (PCA) and Hadamard Transform Domain (HTD) in [24].

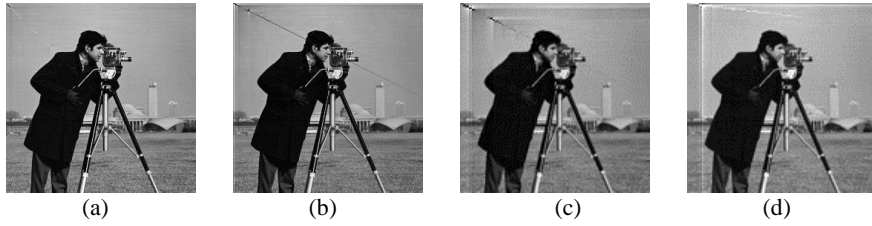


Fig. 10. Recovered watermark from the watermarked image with image resizing: [256×512] (NCC=0.9998) (a), [512×256] (NCC=0.9954) (b), [512×512] (NCC=0.9959) (c), and [1024×1024] (NCC=0.9970) (d)

Table 2. Robustness comparison under various types of attack

Type of attacks	NCC			
	SVD and FWHT [11]	PCA and HTD [24]	HT and SVD (proposed)	Result gap
Without attack	1	1	1	0
Gaussian noise	0.9997 ($\mu=0; \sigma^2=0.1$)	0.9847 ($\mu=0; \sigma^2=0.01$)	0.9692 ($\mu=0; \sigma^2=0.1$)	0.0305
Salt & Pepper noise	0.9945 ($\delta=0.01$)	0.9807 ($\delta=0.01$)	0.9968 ($\delta=0.01$)	0.0023
Poisson noise	0.9950	-	0.9999	0.0049
Speckle noise	0.8835	-	0.9979	0.1144
Rotation	0.5160 ($\theta=40^\circ$)	0.9720 ($\theta=90^\circ$)	1 ($\theta=90^\circ$)	0.028
Cropping	0.7919 ($C=50\%$)	0.9858 ($C=12.5\%$)	0.6677 ($C=12.5\%$)	0.3181
JPEG compression	0.5775 ($Q=50$)	0.9810 ($Q=80$)	1 ($Q=80$)	0.0190
Scaling	-	0.9287 [512×512]	0.9954 [512×512]	0.0667

As presented in Table 2, the proposed method is closely similar to the other methods in the case of watermark extraction without any attack on the watermarked image that the watermark can be recovered with NCC=1. In the case of attacks, the proposed method gives different results. The proposed method underperforms the other methods against Gaussian noise and image cropping. However, the proposed method outperforms and gives better robustness to the other methods against Salt & Pepper noise, Poisson noise, Speckle noise, JPEG compression, image rotation, and image scaling. Based on the results and discussion above, it can be identified that the proposed method could produce the imperceptibility of the SVD image watermarking by applying the Walsh Hadamard transformation on the watermark image and the singular value of the original or host image. This method also produces better robustness in the type of non-geometrical attacks, although outperforms the existing methods in the scaling attacks.

6. Conclusion

The image watermarking method using WH and SVD has been presented in this paper to improve the imperceptibility and robustness of the watermarked image. Experimental results show that image watermarking based on WH and SVD could produce a watermarked image with an imperceptibility average of 47.10 dB, and could recover the watermark with an average NCC close to 1. In the robustness performance, the use of WH transform specifically works well in non-geometrical attacks, such as noise insertion and JPEG compression. In the non-geometrical attacks, the proposed method outperforms the existing other methods that are combining the SVD with FWHT, and also PCA with HTD. In the geometrical attacks, all of the recovered watermarks can be recognized visually by the proposed method to prove the ownership or authentication. The proposed method outperforms in the scaling attacks but underperforms in the image rotation and cropping.

Those limitations can be used as a further problem in further research to improve the use of the Walsh Hadamard transform in SVD image watermarking. Besides, it is also necessary to evaluate the WH and SVD image watermarking on the color image domain, as the color image has slightly different characteristics than the grayscale image. The time complexity analysis of this algorithm is also suggested in further research because this research applies two different data transformations that can lead to more time-consuming on both embedding and extraction processes.

References

1. B o r r a, S., R. T h a n k i, N. D e y. Digital Image Watermarking: Theoretical and Computational Advances. – CRC Press, Taylor & Francis Group, Boca Raton Florida, 2020. DOI: 10.1201/9780429423291.
2. T a h a, D. B., T. B. T a h a. Towards a New Metric for Watermarked Image Assessment. – In: Proc. of 2nd International Conference on Electrical, Communication, Computer, Power and Control Engineering (ICECCPCE'19), 2019, pp. 109-113. DOI: 10.1109/ICECCPCE46549.2019.203757.
3. R a k h m a w a t i, L., W. W i r a w a n, S. S u w a d i. A Recent Survey of Self-Embedding Fragile Watermarking Scheme for Image Authentication with Recovery Capability. – Eurasip J. Image Video Process., Vol. **2019**, No 61, pp. 1-22. DOI: 10.1186/s13640-019-0462-3.
4. H a n, B., J. L i. A New Zero-Watermarking Algorithm Resisting Attacks Based on Differences Hashing. – Cybernetics and Information Technologies, Vol. **16**, 2016, No 2, pp. 135-147.
5. A g a r w a l, N., A. K. S i n g h, P. K. S i n g h. Survey of Robust and Imperceptible Watermarking. – Multimed. Tools Appl., Vol. **78**, 2019, No 7, pp. 8603-8633. DOI: 10.1007/s11042-018-7128-5
6. B a v r i n a, A., V. M y a s n i k o v, R. Y u z k i v. Parameterizable LSB Watermarking Method with Adaptive Key Generation. – In: Proc. of 6th IEEE International Conference on Information Technology and Nanotechnology (ITNT'20), 2020, pp. 1-5. DOI: 10.1109/ITNT49337.2020.9253183.
7. B e g u m, M., M. S. U d d i n. Multiple Image Watermarking with Discrete Cosine Transform. – J. Comput. Commun., Vol. **9**, 2021, No 03, pp. 88-94. DOI: 10.4236/jcc.2021.93006.
8. B e g u m, M., M. S. U d d i n. Implementation of Secured and Robust DFT-Based Image Watermark through Hybridization with Decomposition Algorithm. – SN Comput. Sci., Vol. **2**, 2021, No 3, pp. 1-13. DOI: 10.1007/s42979-021-00608-6.

9. Taha, D. B., T. B. Taha, N. B. Al Dabagh. A Comparison between the Performance of DWT and LWT in Image Watermarking. – Bull. Electr. Eng. Informatics, Vol. **9**, 2020, No 3, pp. 1005-1014. DOI: 10.11591/eei.v9i3.1754.
10. Alshoura, W. H. H., Z. Zainol, J. S. Teh, M. Alawida. A New Chaotic Image Watermarking Scheme Based on SVD and IWT. – IEEE Access, Vol. **8**, 2020, pp. 43391-43406. DOI: 10.1109/ACCESS.2020.2978186.
11. Khanam, T., P. K. Dhar, S. Kowsar, J. M. Kim. SVD-Based Image Watermarking Using the Fast Walsh-Hadamard Transform, Key Mapping, and Coefficient Ordering for Ownership Protection. – Symmetry, Vol. **12**, 2020, No 1, pp. 1-20. DOI: 10.3390/sym12010052.
12. Zermi, N., A. Khaldi, M. R. Kafi, F. Kahlessenane, S. Euschi. An SVD Values Ordering Scheme for Medical Image Watermarking. – Cybern. Syst., Vol. **53**, 2022, No 3, pp. 282-297. DOI: 10.1080/01969722.2021.1983700.
13. Talbi, M., M. S. Bouhlel. Secure Image Watermarking Based on LWT and SVD. – Int. J. Image Graph., Vol. **18**, 2018, No 4, pp. 1-25. DOI: 10.1142/S0219467818500213.
14. Liu, J., J. Huang, Y. Luo, L. Cao, S. Yang, D. Wei, R. Zhou. An Optimized Image Watermarking Method Based on HD and SVD in DWT Domain. – IEEE Access, Vol. **7**, 2019, pp. 80849-80860. DOI: 10.1109/ACCESS.2019.2915596.
15. Marjuni, A., O. D. Nurhayati. Robustness Improvement Against a Non-Geometrical Attacks of Lifting Scheme-based Image Watermarking through Singular Value and Schur Decompositions. – Int. J. Intell. Eng. Syst., Vol. **14**, 2021, No 4, pp. 217-230. DOI: 10.22266/ijies2021.0831.20.
16. Ahmadi, S. B. B., G. Zhang, S. Wei. Robust and Hybrid SVD-Based Image Watermarking Schemes: A Survey. – Multimed. Tools Appl., Vol. **79**, 2020, No 1-2, pp. 1075-1117. DOI: 10.1007/s11042-019-08197-6.
17. Ali, M., C. W. Ahn, M. Pant, P. Siarry. A Reliable Image Watermarking Scheme Based on Redistributed Image Normalization and SVD. – Discret. Dyn. Nat. Soc., Vol. **2016**, No 3263587, pp. 1-15. DOI: 10.1155/2016/3263587.
18. Marjuni, A., M. F. A. Fauzi, R. Logeswaran, S.-H. Heng. An Improved DCT-Based Image Watermarking Scheme Using Fast Walsh Hadamard Transform,” – Int. J. Comput. Electr. Eng., Vol. **5**, 2013, No 3, pp. 271-278. DOI: 10.7763/IJCEE.2013.V5.711.
19. Parvathavarthini, S., R. Shanthakumari. An Adaptive Watermarking Process in Hadamard Transform. – Int. J. Adv. Inf. Technol., Vol. **4**, 2014, No 2, pp. 1-7. DOI: 10.5121/ijait.2014.4201.
20. Zhang, Q., X. Y. Zheng. Walsh Transform and Empirical Mode Decomposition Applied to Reconstruction of Velocity and Displacement from Seismic Acceleration Measurement. – Appl. Sci., Vol. **10**, 2020, No 10, pp. 1-16. DOI: 10.3390/app10103509.
21. Ghazy, R. A., N. A. El-Fishawy, M. M. Hadhoud, M. I. Dessouky, F. E. A. El-Samie. An Efficient Block-by-Block SVD-Based Image Watermarking Scheme. – In: Proc. of 2007 Nat. Radio Sci. Conf., 2007, pp. 1-9. DOI: 10.1109/NRSC.2007.371376.
22. El Houbay, E. M. F., N. I. R. Yassin. Wavelet-Hadamard Based Blind Image Watermarking Using Genetic Algorithm and Decision Tree. – Multimed. Tools Appl., Vol. **79**, 2020, No 37-38, pp. 28453-28474. DOI: 10.1007/s11042-020-09333-3.
23. Lépître, F., C. Fonlupt, S. Verel, V. Marion. Walsh Functions as Surrogate Model for Pseudo-Boolean Optimization Problems. – In: Proc. of Genet. Evol. Comput. Conf. GECCO'19, 2019, pp. 303-311. DOI: 10.1145/3321707.3321800.
24. Moenaddini, E. An Optimized Image Watermarking Scheme in Hadamard Transform Domain for Color Images. – J. Inf. Secur. Res., Vol. **9**, 2018, No 2, pp. 63-77. DOI: 10.6025/jistr/2018/9/2/63-77.

Received: 16.08.2022; Second Version: 28.10.2022; Accepted: 18.11.2022